Supplementary Information

Modular DNA-origami-based nanoarrays enhanced cell binding-affinity through "lock-key" interaction

Miao Mao[1], Zhun Lin[1], Liang Chen[1], Zhengyu Zou[2], Jie Zhang[1], Quanhao Dou[3], Jiacheng Wu[1], Jinglin Chen[1], Minhao Wu[2]*, Li Niu[4]*, Yuanqing Zhang[1]*

[1]School of Pharmaceutical Sciences, Sun Yat-Sen University, Guangzhou, Guangdong 510006, China

[2]Zhongshan School of Medicine, Sun Yat-Sen University, Guangzhou, Guangdong 510080, China

[3]Joint Laboratory of Optofluidic Technology and Systems, National Center for International Research on Green Optoelectronics, South China Academy of Advanced Optoelectronics, South China Normal University, Guangzhou, Guangdong 510006, China

[4]Center for Advanced Analytical Science, School of Chemistry and Chemical Engineering, Guangzhou University, Guangzhou, Guangdong 510006, China

*Corresponding author: Minhao Wu, wuminhao@mail.sysu.edu.cn; Li Niu, lniu@gzhu.edu.cn; Yuanqing Zhang, zhangyq65@mail.sysu.edu.cn

Table of contents

Figures and Tables

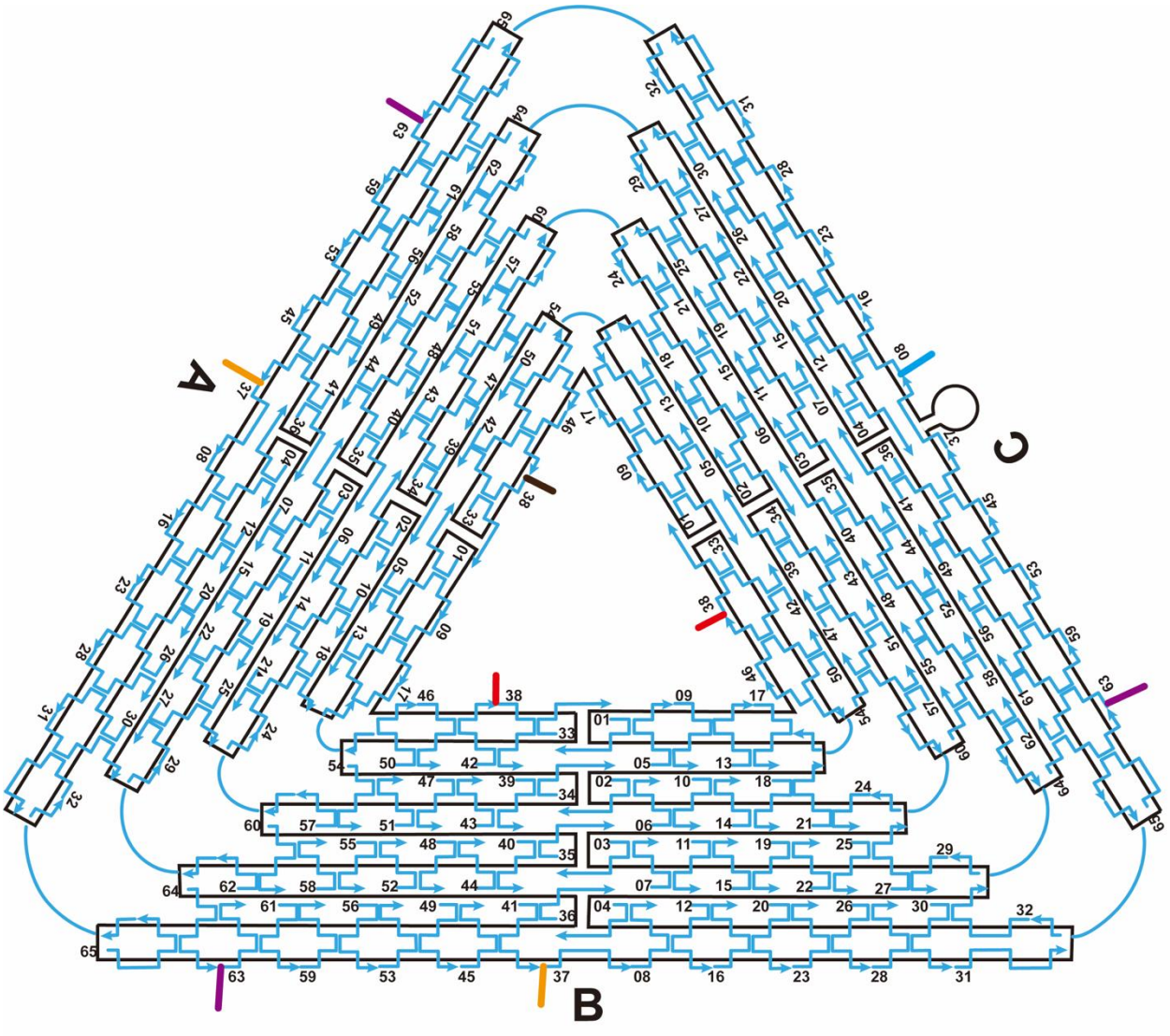

Supplementary Fig. 1. Design of triangular DNA origami. Schematic showing the internal features of the construction of the triangular DNA origami with M13mp18 ssDNA and many staple strands. M13mp18 ssDNA as a scaffold is colored in black, and the staple strands are in blue with individually numbered each strand. The whole complex consists of three major domains which are labeled as A, B, and C. The stand extensions with five colors at nine sites show the location of the different sticky ends, and same color represents the same sticky end.

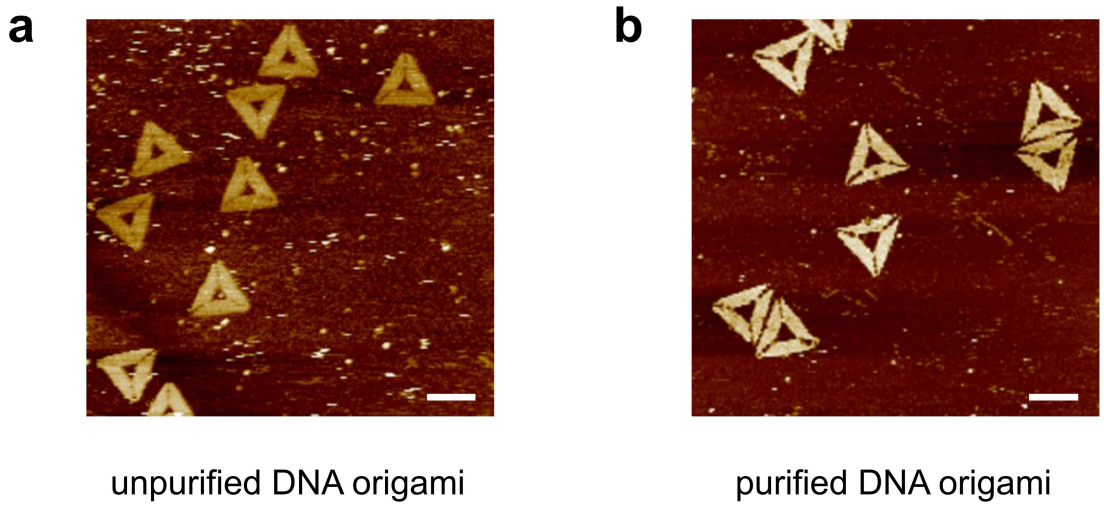

Supplementary Fig. 2. AFM imaging analysis of triangular DNA origami. AFM images of triangular DNA origami before (**a**) and after (**b**) purified. Scale bar: 100 nm.

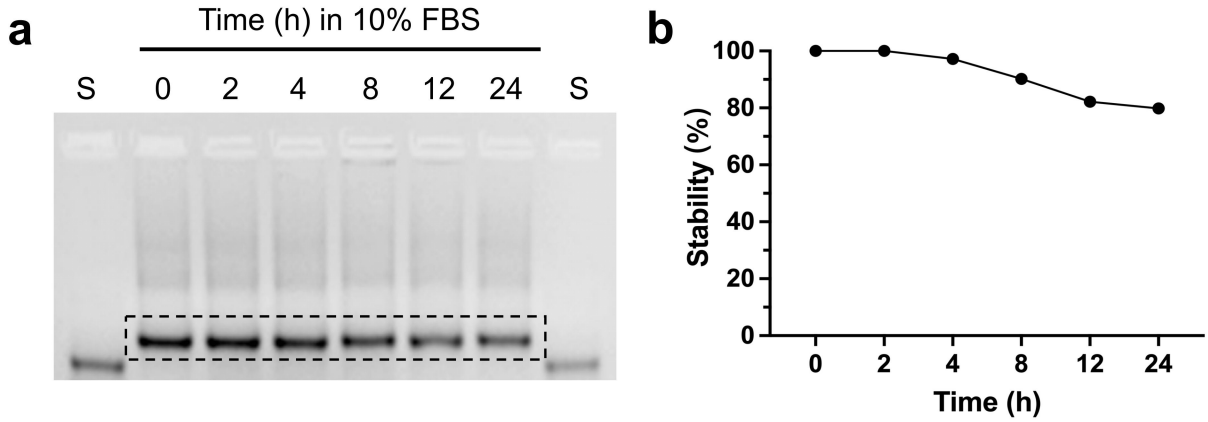

Supplementary Fig. 3. Detection of structural stability of DNA origami. (**a**) 1% agarose gel electrophoresis analysis of DNA origami incubated at 37 ℃ in 10% FBS for different time (0, 2, 4, 8, 12, 24 h). S stands represents M13mp18 scaffold. The rectangular area indicates bands of DNA origami. (**b**) Quantification analysis of the stability of DNA origami structure in (**a**).

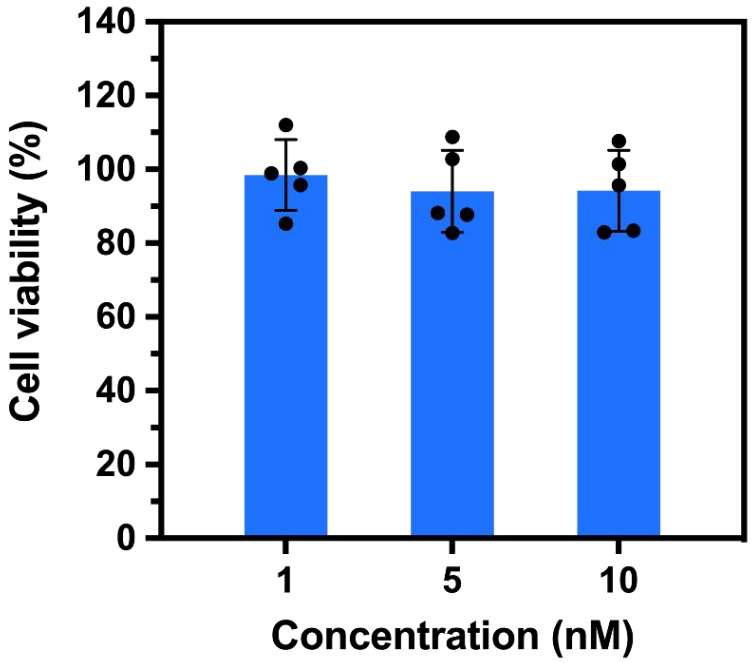

Supplementary Fig. 4. Cytotoxicity assays. The cytotoxicity assessment of different concentrations of DNA origami to MCF-7 cells after incubation for 12 h by CCK-8 assay. Data represent the mean ± s.d. from n=5 independent experiments.

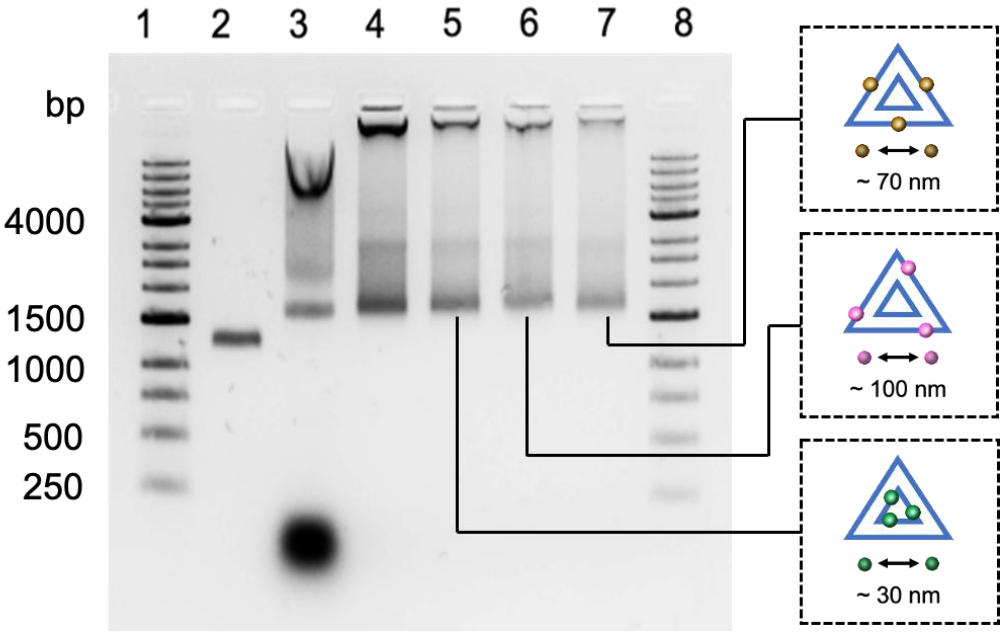

Supplementary Fig. 5. Characterization of formation of DNA nanoarray by 1% agarose gel electrophoresis. From left to right: DNA ladder (lane 1 and lane 8), M13mp18 ssDNA (lane 2), unpurified DNA origami (lane 3), purified DNA origami (lane 4), $O(I)_3$ (lane 5), $O(III)_3$ (lane 6), $O(II)_3$ (lane 7). $O(I)_3$, $O(II)_3$, and $O(III)_3$ represents DNA origami modified with three aptamers with 30-nm, 70-nm, and 100-nm inter-spacing, respectively.

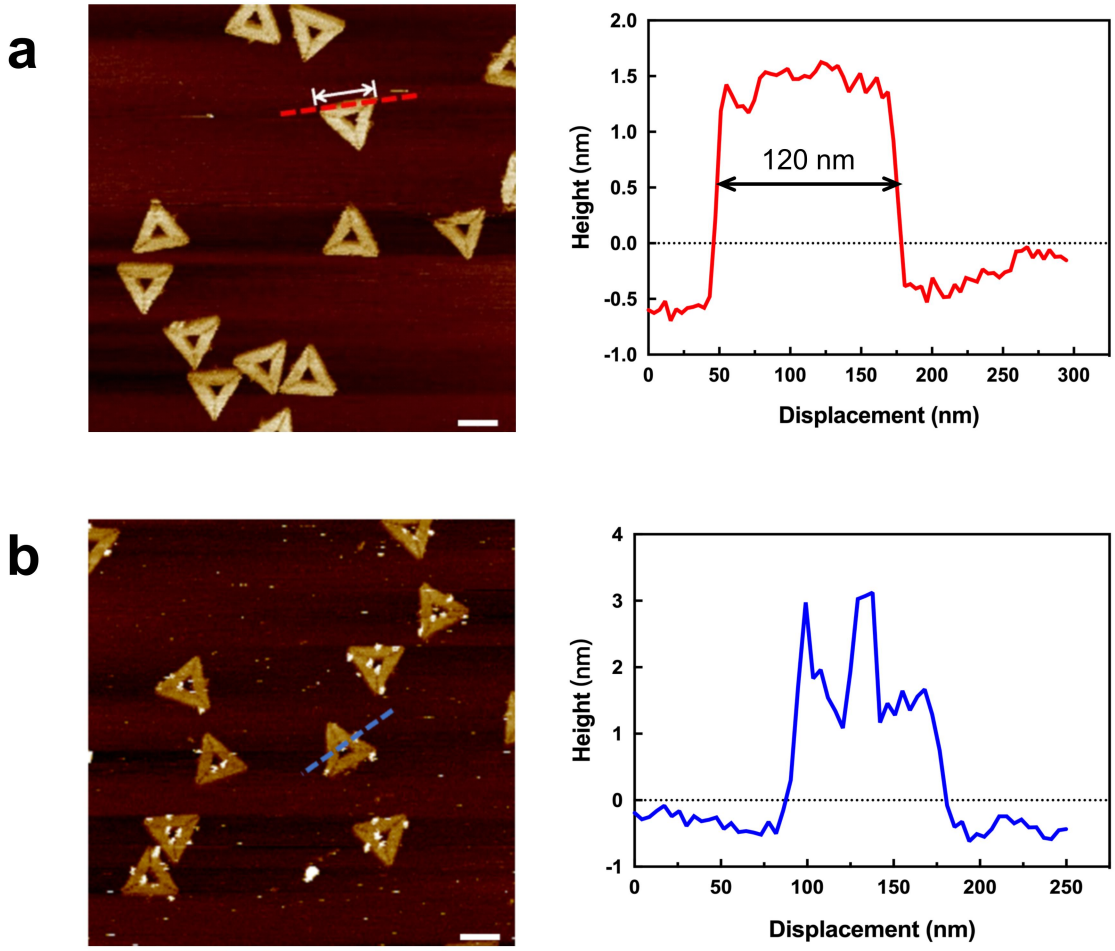

Supplementary Fig. 6. AFM imaging and height analysis of triangular DNA origami. (**a**) Representative AFM images of unmodified DNA origami (left) and its height analysis of line-cross sections (right). Cross-sectional profile of the marker across the dashed red line shows 120-nm edge length of DNA origami. (**b**) Representative AFM images of SA-modified DNA origami (left) and its height analysis of line sections (right). The increasing height of line-cross section (dashed blue line) proves the successful modification of SA. Scale bar: 100 nm.

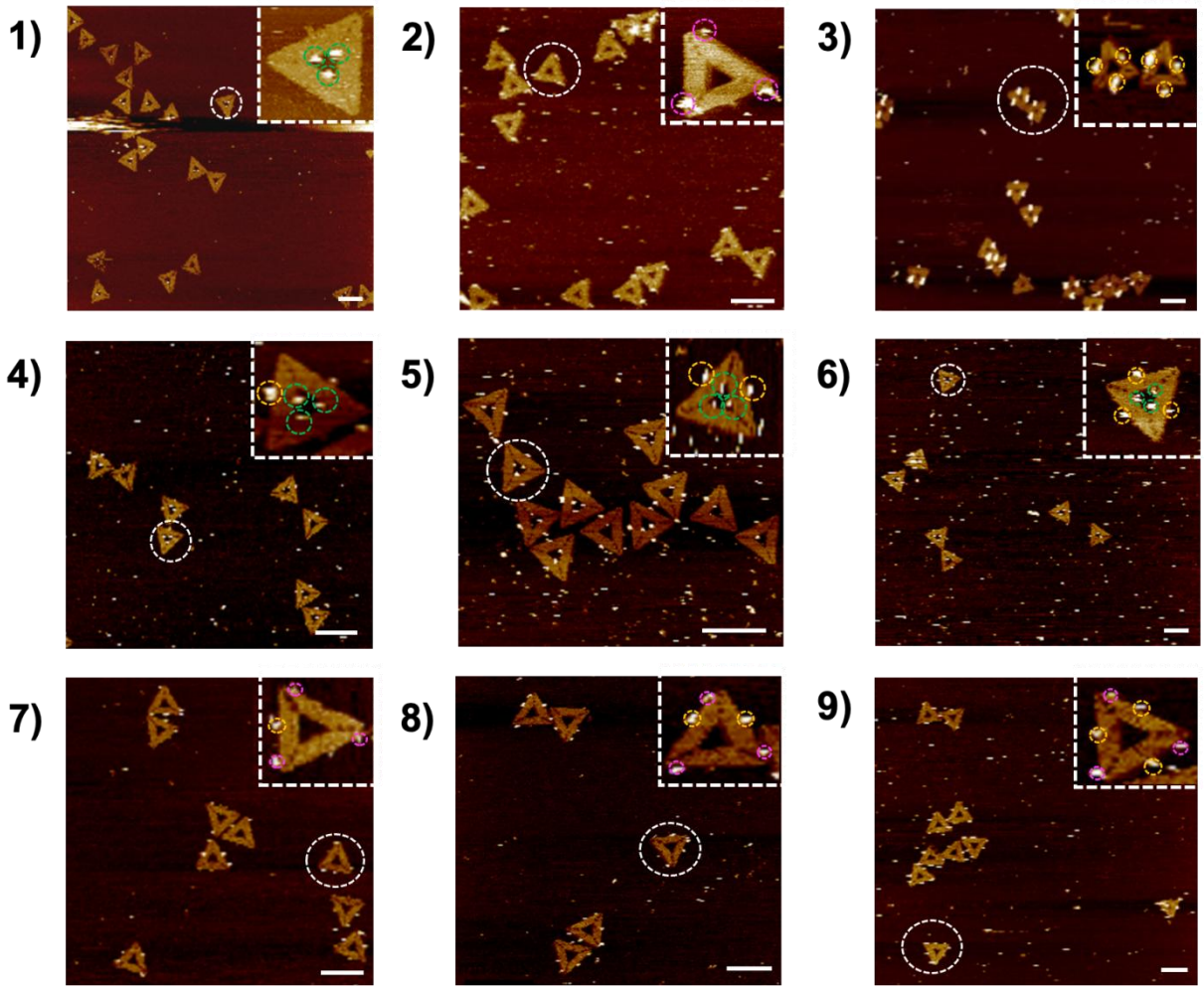

Supplementary Fig. 7. Representative AFM images of modular DNA nanoarrays containing multi-region binding sites. From 1 to 10: $O(I)_3$, $O(III)_3$, $O(II)_3$, $O(I)_3O(II)_1$, $O(I)_3O(II)_2$, $O(I)_3O(II)_3$, $O(III)_3O(II)_1$, $O(III)_3O(II)_2$, $O(III)_3O(II)_3$, respectively. (inset) Enlarged images in the dashed white circle. Scale bar: 150 nm.

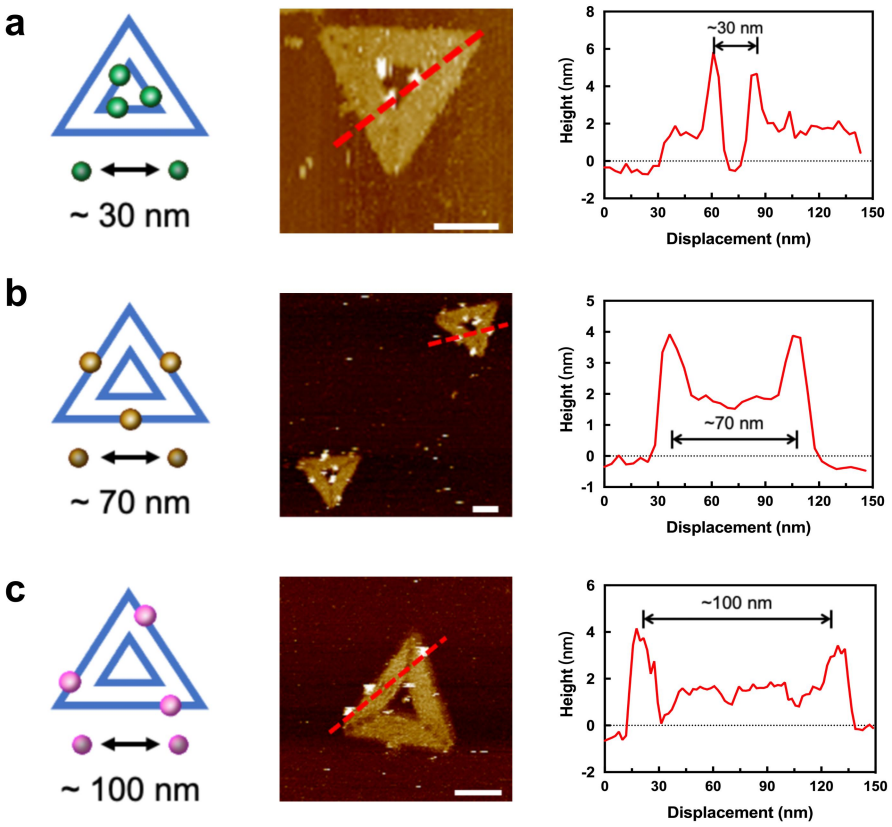

Supplementary Fig. 8. Schematic and representative AFM images of modular DNA nanoarrays with different inter-spacing. (**a**) AFM image of DNA nanoarrays with 30-nm inter-spacing. Cross-sectional profile of the marker across the dashed red line shows that the distance between SA molecules is about 30 nm. (**b**) AFM image of DNA nanoarrays with 70-nm inter-spacing. The distance between SA molecules is about 70 nm (dashed red line). (**c**) AFM image of DNA nanoarrays with 100-nm inter-spacing. The distance between SA molecules is about 100 nm (dashed red line). Scale bar: 50 nm.

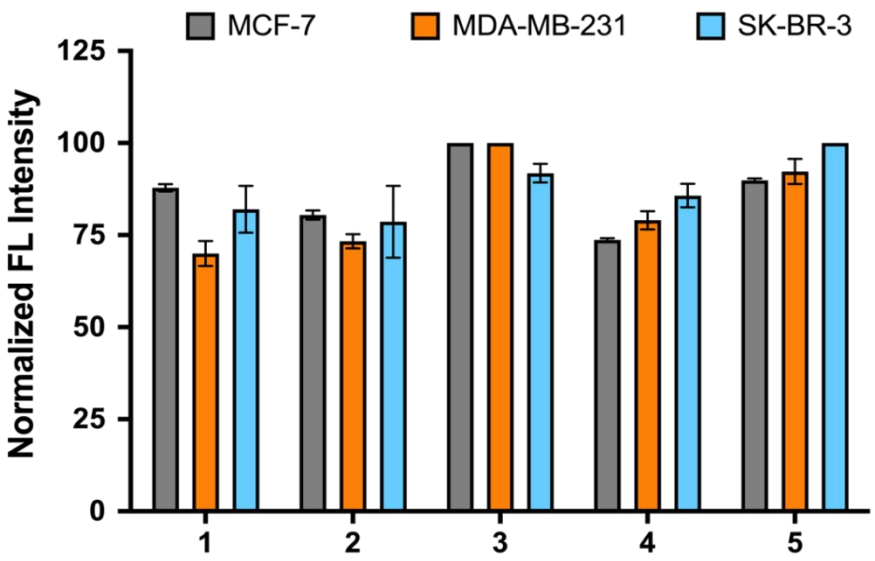

Supplementary Fig. 9. Optimization of aptamer modification of DNA nanoarrays. Normalized fluorescence intensity of MCF-7, SK-BR-3, and MDA-MB-231 cells measured by flow cytometry, after treated with different groups at 4 °C. From left to right: (1) $O(I)_3O(II)_3O(III)_3$ containing 3 Apt-HER2, (2) $O(I)_3O(II)_3O(III)_3$ containing 2 Apt-HER2 and 1 Apt-EGFR, (3) $O(I)_3O(II)_3O(III)_3$ containing 1 Apt-HER2 and 2 Apt-EGFR, (4) $O(I)_3O(II)_3O(III)_3$ containing 3 Apt-EGFR and (5) $O(I)_3O(III)_3$. Data represent the mean ± s.d. from n=3 independent experiments.

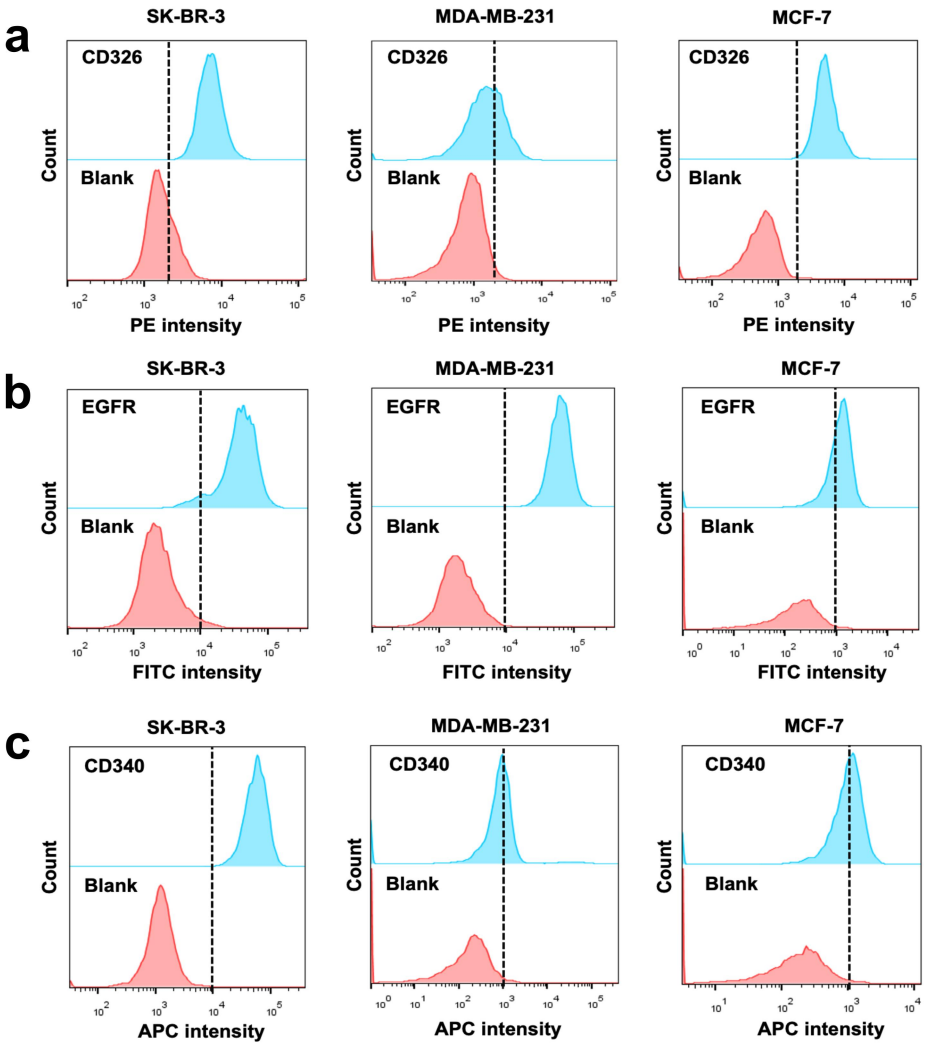

Supplementary Fig. 10. Detection of heterogeneous expression of three breast cancer cell surface proteins. (**a**) After incubated with phycoerythrin (PE)-labeled anti-CD326 (EpCAM) at 4 °C, the fluorescence intensity of MCF-7, SK-BR-3, and MDA-MB-231 cells were detected by flow cytometry. (**b**) After incubated with Alexa fluor 488-labeled anti-EGFR at 4 °C, the fluorescence intensity of MCF-7, SK-BR-3, and MDA-MB-231 cells were detected by flow cytometry. (**c**) After incubated with APC-labeled anti-CD340 (ErbB2/HER2) at 4 °C, the fluorescence intensity of MCF-7, SK-BR-3, and MDA-MB-231 cells were detected by flow cytometry.

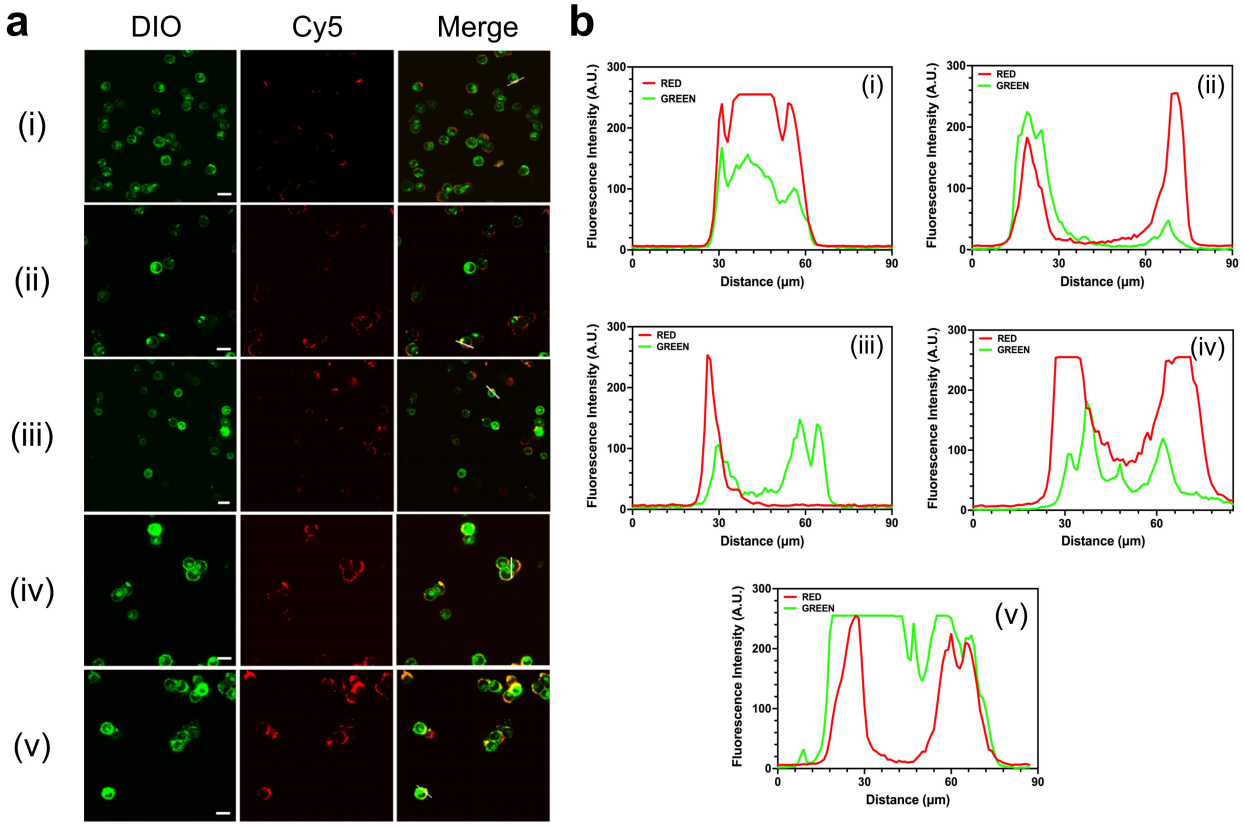

Supplementary Fig. 11. Fluorescence image of MCF-7 cells treated with 10 nM DNA nanoarrays by laser confocal microscope. (**a**) Fluorescence image of DiO stained MCF-7 cells incubated with 10 nM Cy5-labled Apt-EpCAM (i), $O(III)_3$ (ii), $O(I)_3$ (iii), $O(I)_3O(III)_3$ (iv), and $O(I)_3O(II)_3O(III)_3$ (v) at 4 °C. Scale bar: 50 μm. (**b**) The fluorescence intensity of line cross-section analysis of Apt-EpCAM (i), $O(III)_3$ (ii), $O(I)_3$ (iii), $O(I)_3O(III)_3$ (iv), and $O(I)_3O(II)_3O(III)_3$ (v) in (**a**).

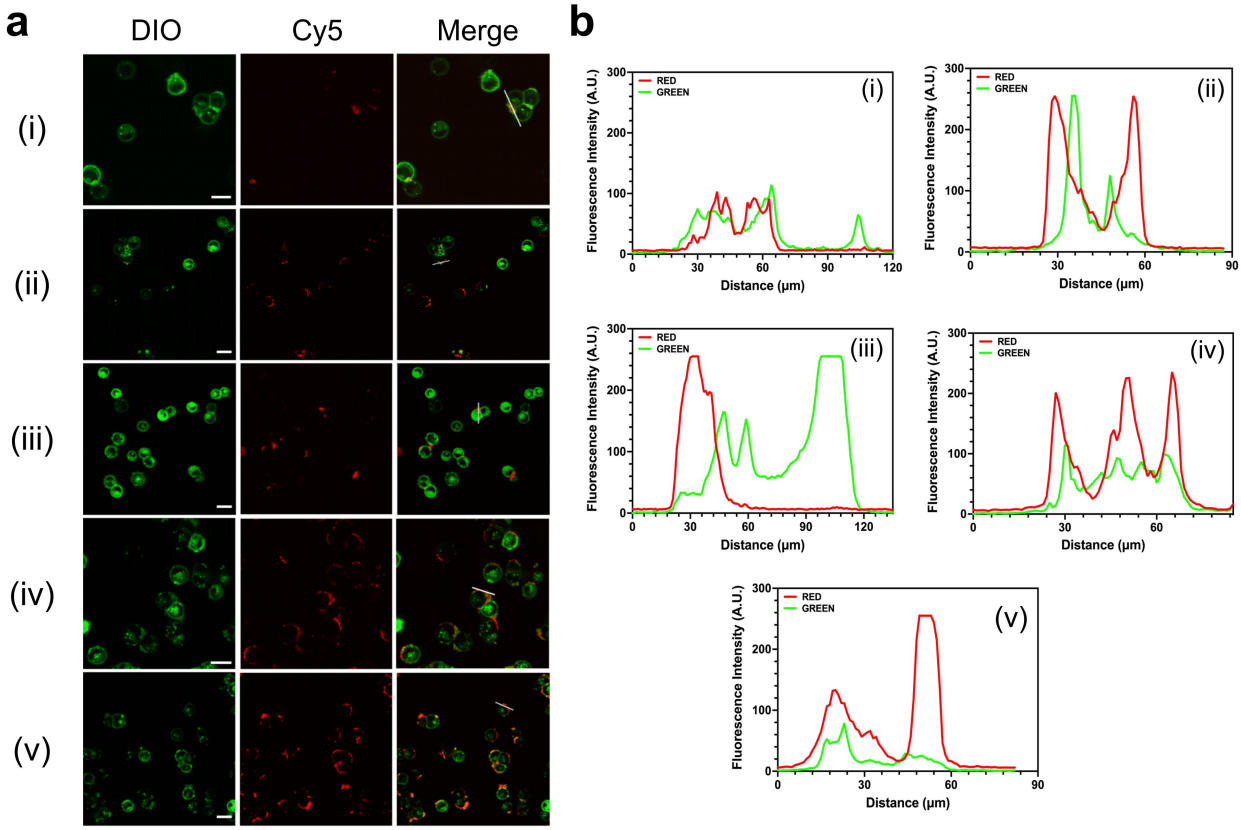

Supplementary Fig. 12. Fluorescence image of MCF-7 cells treated with 5 nM DNA nanoarrays by laser confocal microscope. (**a**) Fluorescence image of DiO stained MCF-7 cells incubated with 5 nM Cy5-labled Apt-EpCAM (i), $O(III)_3$ (ii), $O(I)_3$ (iii), $O(I)_3O(III)_3$ (iv), and $O(I)_3O(II)_3O(III)_3$ (v) at 4 °C. Scale bar: 50 μm. (**b**) The fluorescence intensity of line cross-section analysis of Apt-EpCAM (i), $O(III)_3$ (ii), $O(I)_3$ (iii), $O(I)_3O(III)_3$ (iv), and $O(I)_3O(II)_3O(III)_3$ (v) in (**a**).

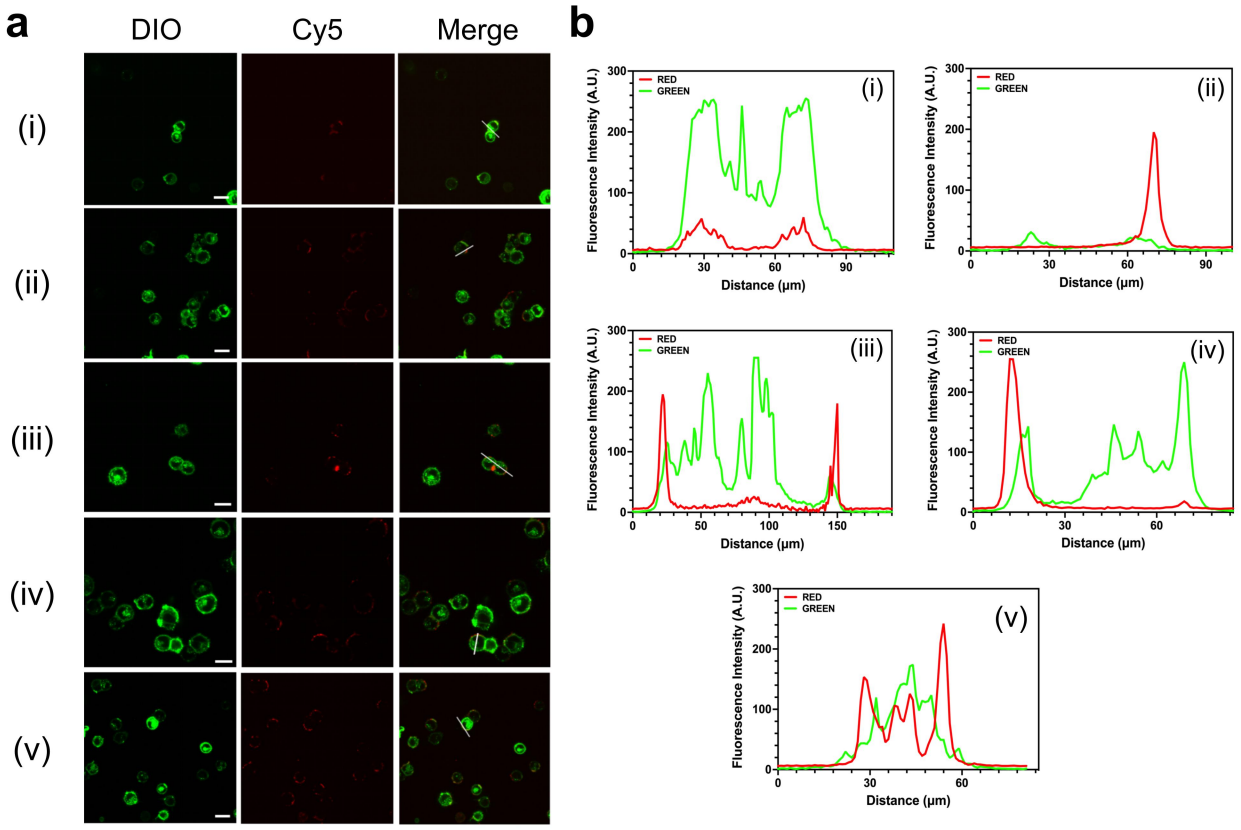

Supplementary Fig. 13. Fluorescence image of MCF-7 cells treated with 1 nM DNA nanoarrays by laser confocal microscope. (**a**) Fluorescence image of DiO stained MCF-7 cells incubated with 1 nM Cy5-labled Apt-EpCAM (i), $O(III)_3$ (ii), $O(I)_3$ (iii), $O(I)_3O(III)_3$ (iv), and $O(I)_3O(II)_3O(III)_3$ (v) at 4 °C. Scale bar: 50 μm. (**b**) The fluorescence intensity of line cross-section analysis of Apt-EpCAM (i), $O(III)_3$ (ii), $O(I)_3$ (iii), $O(I)_3O(III)_3$ (iv), and $O(I)_3O(II)_3O(III)_3$ (v) in (**a**).

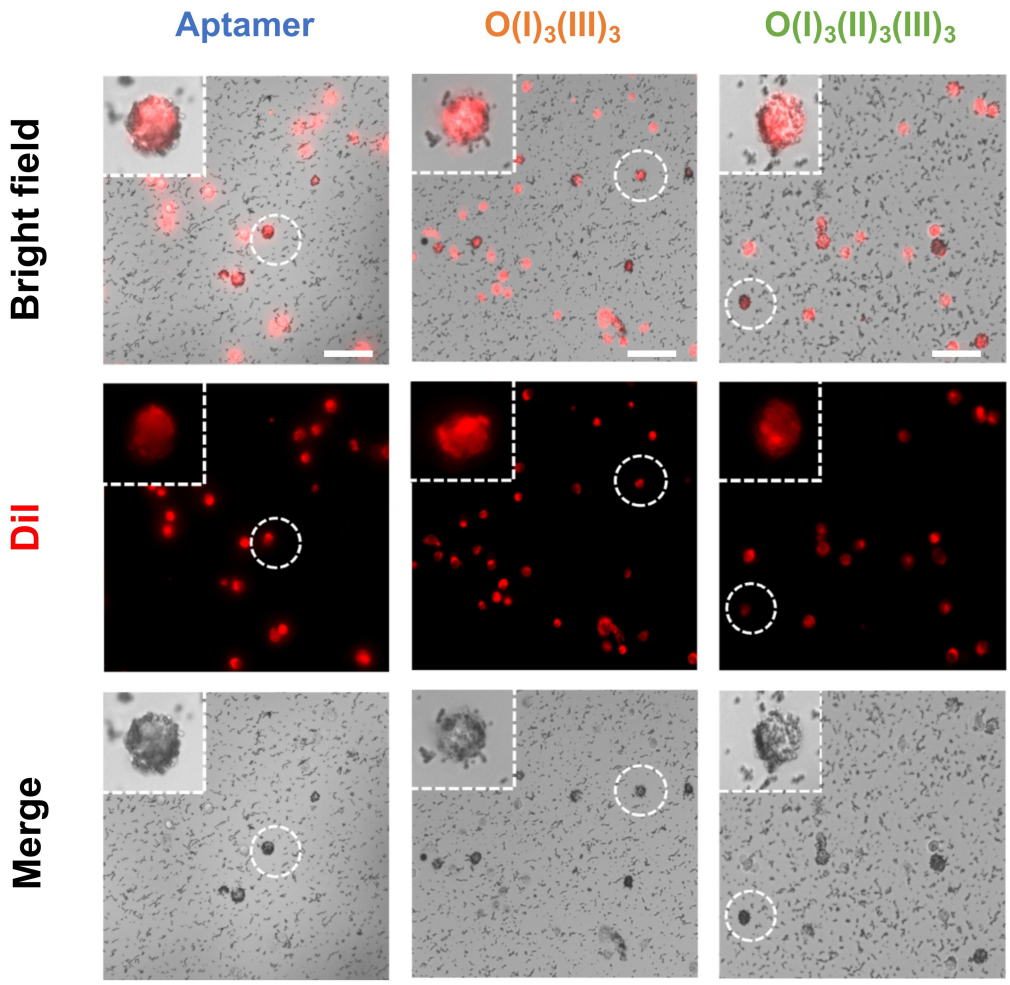

Supplementary Fig. 14. Microscopic image of MCF-7 cells captured by magnetic beads. After incubation with 2 nM biotinylated Apt-EpCAM, $O(I)_3O(III)_3$, and $O(I)_3O(II)_3O(III)_3$, the bright field and fluorescence image of Dil-stained MCF-7 cells captured by the streptavidin magnetic beads. Scale bar: 120 μm.

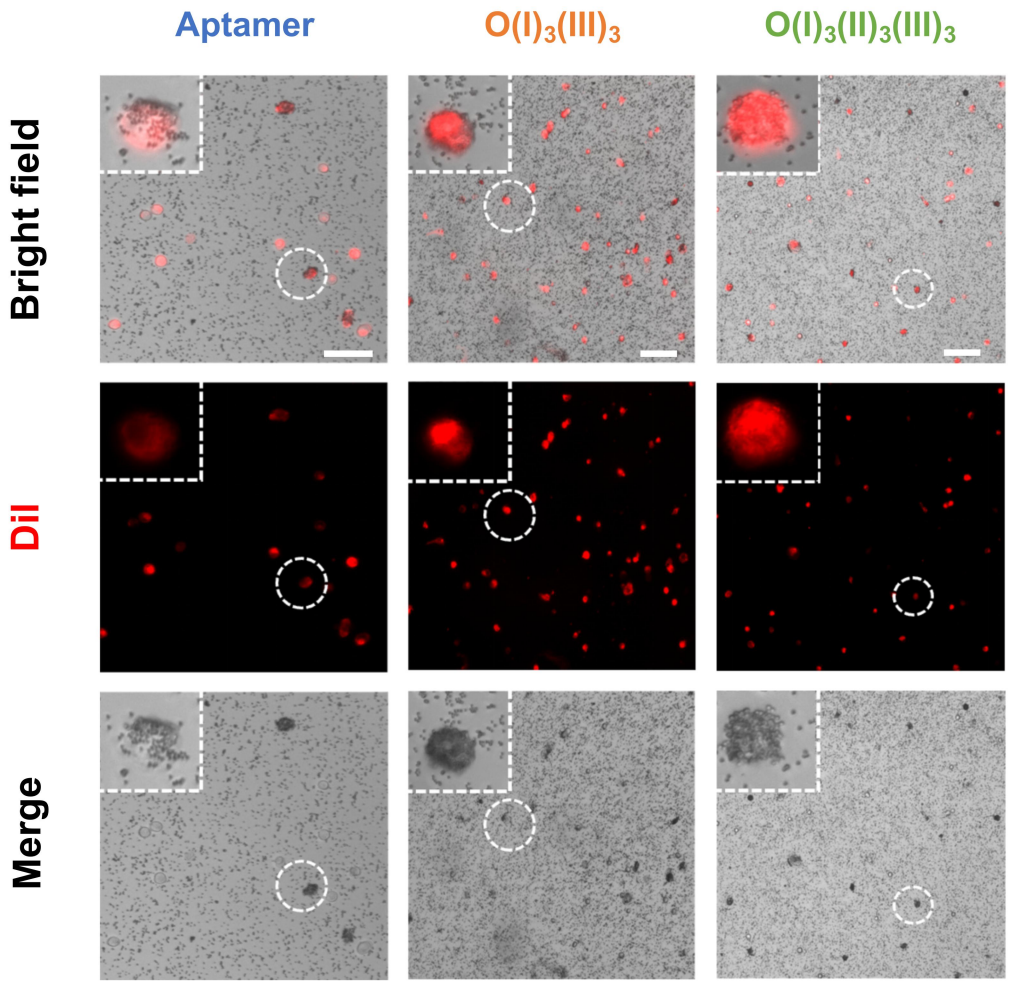

Supplementary Fig. 15. Microscopic image of SK-BR-3 cells captured by magnetic beads. After incubation with 2 nM biotinylated Apt-EpCAM, $O(I)_3O(III)_3$, and $O(I)_3O(II)_3O(III)_3$, the bright field and fluorescence image of Dil-stained SK-BR-3 cells captured by the streptavidin magnetic beads. Scale bar: 120 μm.

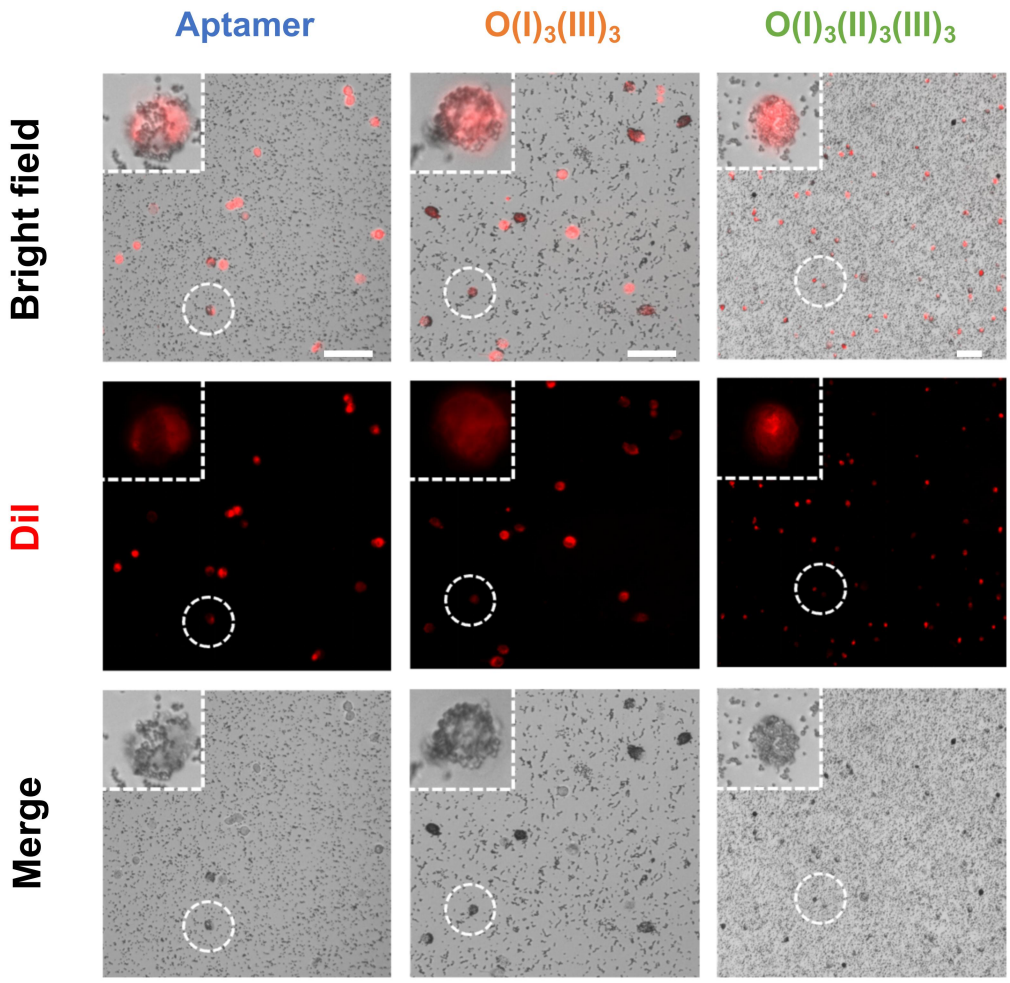

Supplementary Fig. 16. Microscopic image of MDA-MB-231 cells captured by magnetic beads. After incubation with 2 nM biotinylated Apt-EpCAM, $O(I)_3O(III)_3$, and $O(I)_3O(II)_3O(III)_3$, the bright field and fluorescence image of Dil-stained MDA-MB-231 cells captured by the streptavidin magnetic beads. Scale bar: 120 μm.

Supplementary Table 1. Sequences of staple strands containing sticky ends. There are totally 9 staple strands are modified with sticky ends. Note that to prepare DNA origami templates for modular nanoarrays construction, the original unmodified staples are replaced with specific DNA strands containing sticky ends and annealed with the remaining staples.

Name	Sequence of staple strands (5' to 3')
SE1-A38	AGACTCTAATGCAGTCACCAACGCTTTT-AAAACAAAATTAATTAAATGGAAACAGTACATTAGTGAAT
SE2-B38	AATAATAATAATAATAATAATAATTTTT-CCTCAGAACCGCCACCCAAGCCCAATAGGAACGTAAATGA
SE2-C38	AATAATAATAATAATAATAATAATTTTT-GCTCATTTTTTAACCAGCCTTCCTGTAGCCAGGCATCTGC
SE3-A63	AAAAAAAAAAAAAAAAAAAAAAAATTTT-ACGCTAACGAGCGTCTGGCGTTTTAGCGAACCCAACATGT
SE3-B63	AAAAAAAAAAAAAAAAAAAAAAAATTTT-TGGTTTAATTTCAACTCGGATATTCATTACCCACGAAAGA
SE3-C63	AAAAAAAAAAAAAAAAAAAAAAAATTTT-CGATGGCCCACTACGTATAGCCCGAGATAGGGATTGCGTT
SE4-A37	CGCATTCAGGATTCTCAACTCGTATTTT-AGAGAATAACATAAAAACAGGGAAGCGCATTA
SE4-B37	CGCATTCAGGATTCTCAACTCGTATTTT-ACAGGTAGAAAGATTCATCAGTTGAGATTTAG
SE5-C08	AGGTAGGCGGTTGAGGTTTT-TTGACGAGCACGTATACTGAAATGGATTATTTAATAAAAG

Supplementary Table 2. Sequences of biotinylated DNA strands.

Name	Sequence of biotinylated DNA strands (5' to 3')
Biotin-S1	Biotin-TEG-TTT-GCGTTGGTGACTGCATTAGAGTCT
Biotin-S2	Biotin-TEG-TTT-ATTATTATTATTATTATTATTATT
Biotin-S3	Biotin-TEG-TTT-TTTTTTTTTTTTTTTTTTTTTTT
Biotin-S4	Biotin-TEG-TTT-TACGAGTTGAGAATCCTGAATGCG
Biotin-S5	Biotin-TEG-TTT-CCTCAACCGCCTACCT
Biotin-A31	Biotin-TEG-TTTTTT- TATCTTACCGAAGCCCAAACGCAATAATAACGAAAATCACCAG

Supplementary Table 3. Sequences of input DNA strands containing sticky ends.

Name	Sequence of input DNA strands (5' to 3')
S1-EpCAM	GCGTTGGTGACTGCATTAGAGTCTTTTTT-CACTACAGAGGTTGCGTCTGTCCCACGTTGTCATGGGGGGTTGGCCTG
Cy5-S1-EpCAM	Cy5-GCGTTGGTGACTGCATTAGAGTCTTTTTT-CACTACAGAGGTTGCGTCTGTCCCACGTTGTCATGGGGGGTTGGCCTG
S2-EpCAM	ATTATTATTATTATTATTATTATTTTTTT-CACTACAGAGGTTGCGTCTGTCCCACGTTGTCATGGGGGGTTGGCCTG
Cy5-S2-EpCAM	Cy5-AAAAAAAAAAAAAAAAAAAAAAATTTT-ACGCTAACGAGCGTCTGGCGTTTTAGCGAACCCAACATGT
S3-EpCAM	TTTTTTTTTTTTTTTTTTTTTTTTTTTTT-CACTACAGAGGTTGCGTCTGTCCCACGTTGTCATGGGGGGTTGGCCTG
Cy5-S3-EpCAM	Cy5-TTTTTTTTTTTTTTTTTTTTTTTTTTTTT-CACTACAGAGGTTGCGTCTGTCCCACGTTGTCATGGGGGGTTGGCCTG
S4-HER2	TACGAGTTGAGAATCCTGAATGCGTTTT-GCAGCGGTGTGGGGGCAGCGGTGTGGGGGCAGCGGTGTGGGG
S4-EGFR	TACGAGTTGAGAATCCTGAATGCGTTTT-TACCAGTGCGATGCTCAGTGCCGTTTCTTCTCTTTCGCTTTTTTTGCTTTTG AGCATGCTGACGCATTCGGTTGAC
S5-HER2	CCTCAACCGCCTACCTTTTT-GCAGCGGTGTGGGGGCAGCGGTGTGGGGGCAGCGGTGTGGGG
S5-EGFR	CCTCAACCGCCTACCTTTTT-TACCAGTGCGATGCTCAGTGCCGTTTCTTCTCTTTCGCTTTTTTTGCTTTTG AGCATGCTGACGCATTCGGTTGAC

Supplementary Table 4. Summary of dissociation kinetics of the *koff* value and the half-lives ($t_{1/2}$).

Multimers	*koff* ($10^{-4}s^{-1}$)	$t_{1/2}$ (min)	R^2
Apt-EpCAM	0.085	8.138	0.9691
$O(I)_3O(III)_3$	3.50	32.98	0.9769
$O(I)_3O(II)_3O(III)_3$	2.25	51.35	0.9462